

Thermal Considerations for Hydroformed Reflectors

William A. Imbriale and Eric Gama
Jet Propulsion Laboratory, California Institute of Technology
4800 Oak Grove Dr.
Pasadena, CA 91109
818-354-5172 and 818-354-1396
William.A.Imbriale@jpl.nasa.gov and Eric.Gama@jpl.nasa.gov
Kenneth S. Smith
Alliance Spacesystems, Inc.
1250 Lincoln Ave., Suite 100
Pasadena, CA 91103
626-296-1373 x125
ksmith@asi-space.com
Roger Shultz
Schultz Associates
2408 Roundhill Dr.
Alamo, CA 94507
925-820-2151
schultz_assoc@pipeline.com

Abstract—One antenna design under consideration^{1,2} for both the next generation Deep Space Network (DSN) array and the Square Kilometer Array (SKA) project is a *hydroformed symmetrically shaped dual reflector system*. Hydroforming is the process of forming aluminum to a rigid and precise mold by using a fluid or gas under pressure. Three 6-meter hydroformed reflectors with rms less than 8 mils (0.2 mm) have been delivered to JPL.

One concern about the high-frequency performance of these antennas is the surface deformation caused by thermal gradients. The rms surface requirement for the combined as manufactured shape plus thermal and gravity deformations is 10.7 mils (0.27mm). The first assembled dish was not painted (bare aluminum only) and measurements of surface rms under mid-day sun showed an rms exceeding 14 mils (0.36mm) rms. After application of the triangle no. 6 diffusive white paint typically used on JPL reflectors, the rms under similar conditions was reduced to less than the 10.7 mil (0.27mm) specification. This paper discussed the thermal design and performance of the 6-meter hydroformed reflector as well as projecting the performance of the SKA 12-meter antenna.

TABLE OF CONTENTS

1. INTRODUCTION	1
2. REFLECTOR DESIGN	2
3. GRAVITY AND THERMAL DISTORTIONS	2
4. THERMAL MEASUREMENTS	4
5. THERMAL DISTORTION ANALYSIS	6
6. COMPARISON OF MEASURED AND CALCULATED THERMAL DISTORTIONS	6

7. PROPOSED 12-METER HYDROFORMED REFLECTOR FOR US SKA	8
8. THERMAL DESIGN	10
9. THERMAL RESULTS	11
10. CONCLUSIONS	12
ACKNOWLEDGMENT	12
REFERENCES	12
BIOGRAPHY	13

1. INTRODUCTION

Development of very large arrays of small antennas has been proposed as a way to increase the downlink capability of the NASA Deep Space Network (DSN) by two or three orders of magnitude thereby enabling greatly increased science data from currently configured missions or enabling new mission concepts [1]. It is also the design proposed by the US for the SKA (Square Kilometer Array), the next generation radio astronomy telescope [2]. One antenna design under consideration for both the DSN array and the SKA project is a *hydroformed symmetrically shaped dual reflector system*. Hydroforming is the process of forming aluminum to a rigid and precise mold by using a fluid or gas under pressure. Three 6-meter hydroformed reflectors with rms less than 0.2 mm have been delivered to JPL. They have been integrated with a backup structure that utilizes 9 equally spaced aluminum struts connecting a center yoke to the rim of the dish. The pedestal consists of a central pipe tucked under the dish with a central bearing for azimuth motion and a jackscrew for elevation control. These antennas have been assembled and are currently undergoing testing [3].

One concern about the high-frequency performance of these antennas is the surface deformation caused by thermal gradients. The rms surface requirement for the combined as

¹ 0-7803-9546-8/06/\$20.00© 2006 IEEE
² IEEEAC paper #1397, Version 2, Updated Dec. 19 2005

manufactured shape plus thermal and gravity deformations is 10.7 mils. The first assembled dish was not painted (bare aluminum only) and measurements of surface rms under mid-day sun showed an rms exceeding 14 mils rms. After application of the typical triangle white paint used on JPL reflectors, the rms under similar conditions was reduced to less than the 10.7 mil specification. This paper discussed the thermal design and performance of the 6-meter hydroformed reflector as well as projecting the performance of the SKA 12-meter antenna.

2. REFLECTOR DESIGN

The critical technology in the mechanical system is the hydroformed dish. It has been highly developed for use in production of low-cost reflectors for satellite communications and thousands of antennas in the 1 to 4 meter range have been manufactured. The advantages are: 1) High rigidity due to the one-piece aluminum shell (consider the stiffness of thin metal bowls or woks compared to the stiffness of flat sheets) 2) Accuracy largely determined by the mold rather than human error (the repeatability of the process was verified by fabricating 3 dishes with an rms of less than 0.2 mm) and 3) Low costs for both raw material and labor.

For the DSN breadboard, the dish aperture is 6.048 m or 20 ft (see Figure 1 for the hydroformed shell). The dish is connected to a rigid Truss Structure at two places. The dish is hard mounted to the Truss Structure at its center. Spars connect the rim of the Dish to the rear of the Truss Structure. The Truss Structure is connected to the Petal Yoke at the elevation pivot point. There is a linear actuator or Jackscrew mechanism attached to the rear of the Yoke. As the Jackscrew extends or contracts the elevation of the Main Dish is changed. The Yoke is connected to the Petal Base through a Slew Bearing, with gears on the outer ring. Two opposing motors, mounted inside the Yoke, drive the Azimuth Axis. The Dish, Truss Structure and Spars are made of aluminum. The Yoke and Pedestal Base are made of steel. The total weight of the antenna is approximately 8500 lbs. See Figure 2 for a drawing and Figure 3 for a picture of the complete antenna.

3. GRAVITY AND THERMAL DISTORTIONS

Surface accuracy of the dish after manufacturing must be less than 0.2 mm rms. For either gravity, wind or temperature the change in rms cannot be greater than 0.13 mm.

The dish was assembled inside a high-bay building and initial measurements were made of the as manufactured shape as well as the gravity performance as a function of elevation angle. Figure 4 is a picture of the front surface of the dish with the targets used for the photogrammetry measurements of the dish surface. This is prior to installing

the feed, subreflector and subreflector support. The surface RMS is 0.3256 mm (12.82 mils). The dish was measured approximately every 22 degrees down to an elevation of 20 degrees (the lowest elevation angle that could be accommodated inside the building). There were two sets of measurements and the data is summarized in Table 1. Figure 5 is a graph of the difference between 90 and 20 degrees elevation. The RMS is less than 0.05 mm (2 mils). As seen from the table and graph, the dish exhibits excellent performance as a function of elevation angle.

Table 1. RMS performance as a function of elevation angle

Elevation Angle (degrees)	Measurement 1		Measurement 2	
	RMS (mils)	RMS (mm)	RMS (mils)	RMS (mm)
20.0	12.67	0.3218	12.56	0.3213
32.5	12.45	0.3162	12.64	0.3211
45.0	12.91	0.3279	12.44	0.3160
67.5	12.68	0.3221	12.66	0.3216
90.0	12.19	0.3096	12.82	0.3256

The subreflector and subreflector supports were installed and the dish re-measured at 45 degrees and the RMS was 0.3239 mm (12.75 mils), virtually the same as the no subreflector case. The antenna was partially disassembled, transported to the JPL Mesa Test Range and reassembled (Figure 3). An initial measurement was made at nighttime (elevation 45 degrees) since it was an isothermal condition similar to the original assembly. The RMS was 0.4531 mm (17.84 mils), indicating that there was some degradation caused during transport and reassembly. This problem was ultimately fixed by shimming the reflector rim to be in a plane. However, the dish was also measured at 10 degrees elevation and the difference from 45 degrees elevation was only 0.036 mm (1.4 mils) continuing the excellent performance for gravity effects.



Figure 1. Hydroformed Dish

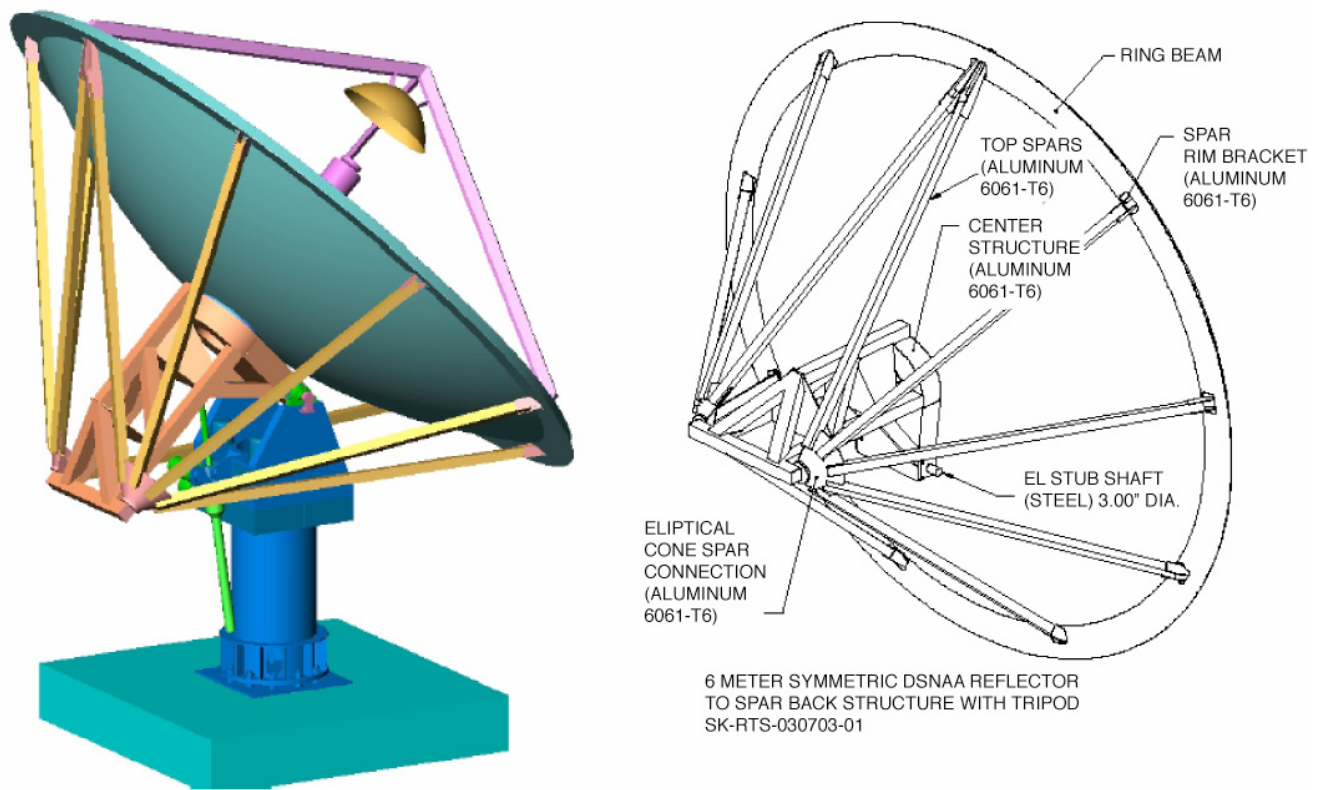


Figure 2. The 6-meter Breadboard Antenna Drawing



Figure 3. The 6-meter Breadboard Antenna



Figure 4. Front Surface with Photogrammetry Targets

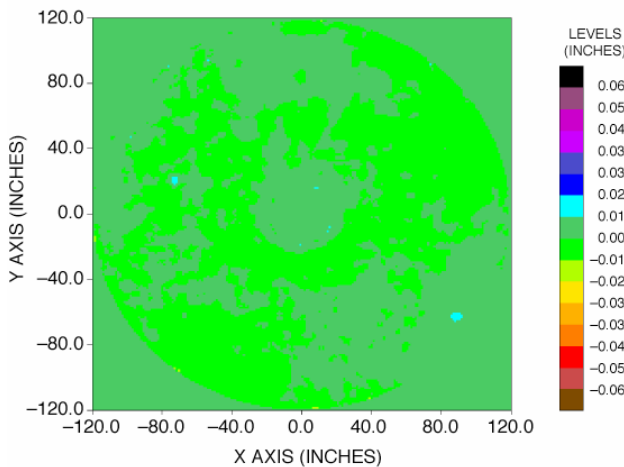


Figure 5. Difference Between 90 and 20 Degrees Elevation

A measurement was made with the dish in full sun and best-fit surface rms was 0.574 mm (22.60 mils) indicating a significant thermal effect. This thermal variation was expected since the dish is not painted with the traditional triangle no. 6 diffusive white paint. There was a desire to measure dishes with and without paint to determine if the cost of painting the surface could be eliminated. The difference between the full sun and nighttime case is shown in Figure 6. The RMS of the difference between the two cases is 0.3352 mm (13.2 mils), which exceeds the thermal requirement, indicating that it will be necessary to paint the dishes.

4. THERMAL MEASUREMENTS

Photogrammetric data of the surface of Antenna 1 (ANT-1) and Antenna 2 (ANT-2) located on the Mesa Antenna Range (MAR) at the Jet Propulsion Laboratory (JPL) were recorded through several different days to characterize the

surface as it experiences a typical thermal cycle throughout the day.

Temperatures on the various parts of the antenna structure were obtained through the use of an array of thermocouples. J-type thermocouples were used and adhered directly onto the surface of the antenna surface and spar back-up structure to record temperature during photogrammetric data acquisition (see Figure 7).

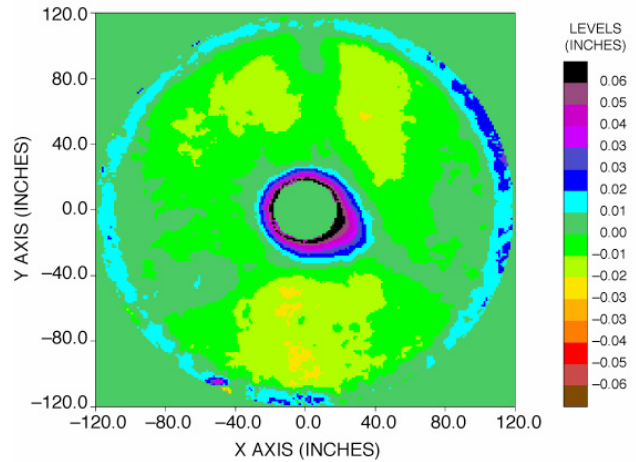
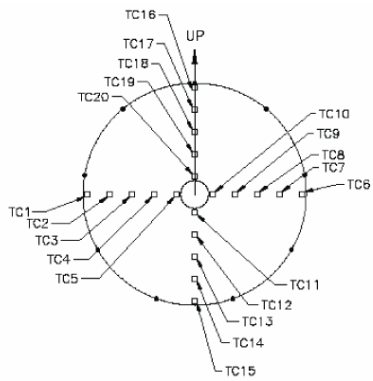


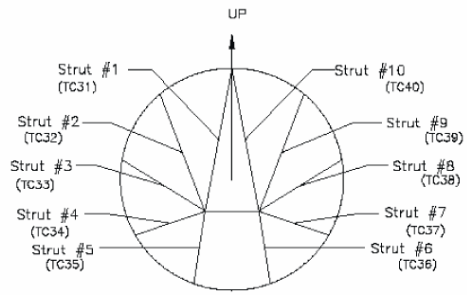
Figure 6. Difference Between Full Sun and Nighttime for Unpainted Dish

Surface data was obtained through the use of photogrammetry. In order to generate a data set that provided a suitable representation of the antenna surface, adhesive backed reflective targets were applied directly to the surface. These targets were 6 mm in diameter and were spaced at roughly 6 inches center-to-center (see Figure 8).

Two challenges had to be dealt with while trying to obtain the photogrammetric data. First, the bright sunlight during the middle part of the day combined with the photogrammetry camera strobe/flash made the targets as well as the surface surrounding the targets too bright for the photogrammetric software to be able to differentiate between the white antenna surface and the reflective target. Secondary effects were the overdriving or over-illumination of the data, which also blurred the boundary lines differentiating the surface from the targets. This problem was resolved through the use of a solar filter and an auxiliary strobe/flash. The filter was able to reduce the amount of reflected light from the white surface while sufficiently illuminating the targets. Second, the challenge of cold weather in combination with the ability of the cold aluminum materials to attract atmospheric moisture posed a problem while trying to obtain lower temperature surface data. Although not as big a problem as the first, the moisture on the targets made for long days and nights of data acquisition.

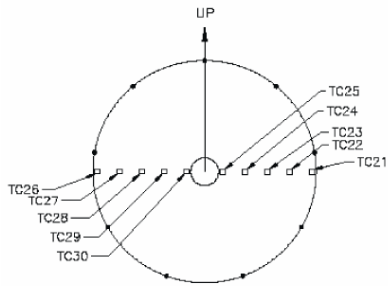


LOOKING INTO DISH FROM FRONT: EL ANGLE = 0 (Horizon)



LOOKING AT ANTENNA FROM REAR OF DISH: EL ANGLE = 0 (Horizon)

Note: There are two additional thermocouples being recorded. These are TC41 and TC42 in the excel data sheet. TC41 is located in the air near the reflector front surface. TC42 is located in the air next to the cryopump housing near the ground. These two thermocouples give us ambient air temperature.



LOOKING AT DISH FROM REAR: EL ANGLE = 0 (Horizon)

Figure 7. Thermocouple Locations on Antenna



Figure 8. Typical layout of Thermocouples and Photogrammetric Targets

5. THERMAL DISTORTION ANALYSIS

Finite element analysis was used to estimate deformations of the reflector caused by measured thermal gradients. An MSC.Nastran finite element model of the 6-meter antenna and support structure was developed by JPL (see Figure 9), consisting of 17,085 nodes and 16,766 elements. The reflector was modeled with shell elements, and the remainder of the structure was modeled with beam elements. The active surface of the reflector was meshed with 2,340 nodes.

After development and checkout of the finite element model, the analysis proceeded in three steps.

Interpolation of Temperatures

Temperatures were measured at 40 locations on the structure. For any assumed temperature profile, these 40 temperatures were interpolated to the full finite element model to allow thermal distortion analysis to take place. For the reflector, temperatures were interpolated separately on the front and back surface, so that the effects of thermal gradients through the skin could be included.

Temperature interpolation from coarse measurements to a finely meshed model can be performed in a number of ways. The best approach is to perform a thermal conduction analysis on the finite element model, with enforced temperatures at the nodes with thermocouples. The analysis would then calculate the temperatures at all other nodes in the model. This approach requires that proper thermal conduction properties for all elements and connections be included in the finite element model.

For the present effort, a simpler approach was taken, based only on geometry. Each of the support struts was assumed to have a uniform temperature. On the reflector surface, nodal temperatures were interpolated in a cylindrical coordinate system. In the radial coordinate, linear interpolation was used. In the angular coordinate, interpolation shape functions were half-cosine functions between adjacent measurement positions. Figure 10 shows a typical interpolated temperature profile (temperature differences from test measurements at different times).

Distortions for Unit Temperature Cases

The interpolation procedure described above is linear in the sense that the interpolated temperatures are linearly dependent on the prescribed (measured) temperatures. The distortions resulting from any temperature profile are also linearly dependent on the interpolated temperatures. Therefore it is possible to reconstruct the deformation from any arbitrary temperature profile from the deformations computed from unit temperature cases.

Each unit case consisted of a temperature change of 1 degree at one thermocouple location, with the other 39 thermocouple locations having no temperature change. There were 40 such cases, one for each thermocouple. For each case, the temperatures were interpolated to the full finite element model, and structural deformation from thermal expansion was computed. The (x,y,z) displacements of all 2,340 reflector surface nodes were tabulated for each case. The final product of this analysis was a 7,020 by 40 matrix of surface deformations versus thermocouple temperature differentials. (3 coordinates at 2,340 nodes gives 7,020 displacements.)

Distortions for Measured Temperature Profiles

Once the matrix was generated for unit cases, it was possible to calculate surface displacements for any arbitrary temperature profile by a simple matrix multiplication. (Multiplying the 7,020 by 40 matrix by a vector of 40 temperature differences gives 7,020 displacements.) Figure 11 shows a typical normal displacement profile produced by this procedure. The distortions correspond to the temperatures shown in Figure 10. The displacements are plotted after subtracting the best-fit rigid body motion of the reflector, which would not be detected by photogrammetry measurements.

6. COMPARISON OF MEASURED AND CALCULATED THERMAL DISTORTIONS

Photogrammetry measurements were taken on the unpainted Antenna #1 starting before sunrise and every 2 hours thereafter until sunset for two consecutive days. The antenna itself was positioned at approximate angles of 229 degrees in azimuth and 15 degrees in elevation on day 1 and 82 degrees elevation on day 2. This positioning allowed for maximizing direct sunlight on the reflector surface without affecting the back structure and spars too greatly as well as for the most efficient photogrammetry position/access. In this position the back structure and struts remained in the shadow of the reflector for the majority of the measurements runs taken. Early morning had partial sun as well as late afternoon/sunset; all other measurement runs had full sun on the reflector. Both the temperatures and rms distortion are shown on Figure 12. The average front, rear and strut temperatures are shown. Also plotted was the difference between the average front and strut temperatures. The theoretical distortions track very accurately this temperature difference, with the distortion almost 1 mil rms for each degree of temperature difference. The rms derived from the photogrammetry is also shown on the plot, and for the most part has the same characteristic as the computed rms.

Antenna #1 was painted with the standard JPL white paint and the measurement repeated for the 15-degree elevation case and the results show on Figure 13. Observe that, even though it was a much hotter day, the difference between the

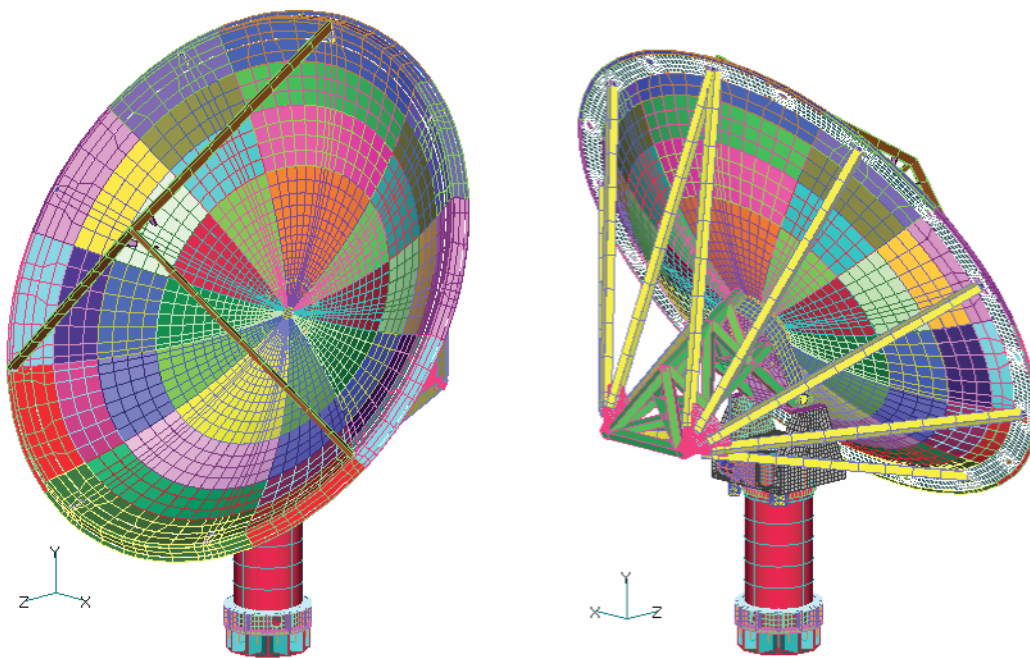


Figure 9. A Finite Element Model of the 6-meter Hydroformed Reflector and Support Structure

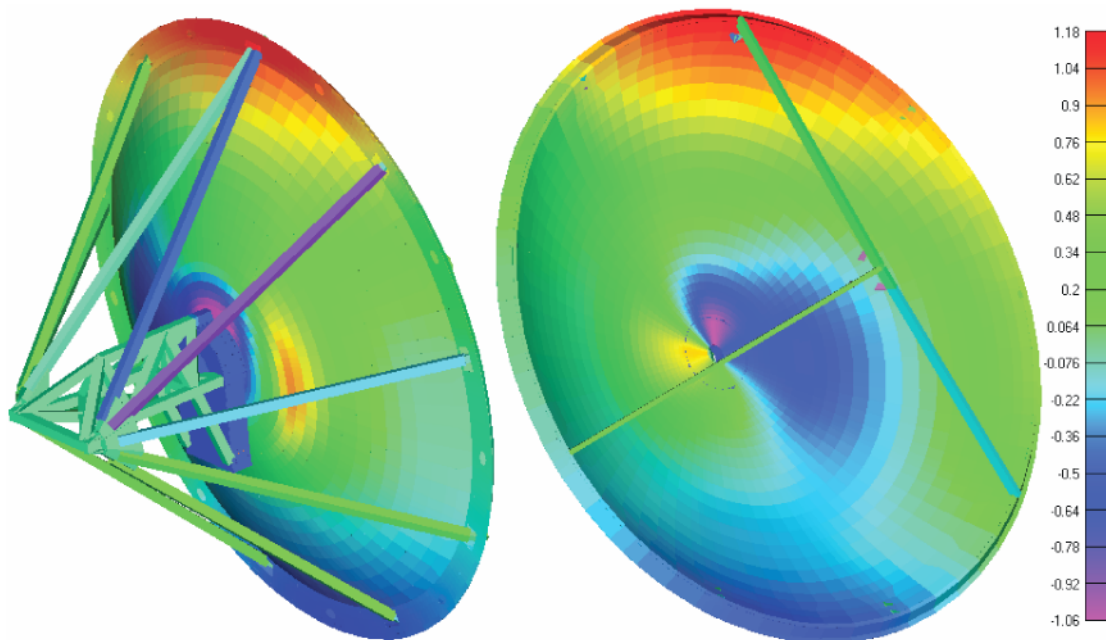


Figure 10. Typical Interpolation from Discrete Temperature Measurements to the Full Finite Element Model. Note that front and back reflector temperatures are separately interpolated. Units are degrees Fahrenheit.

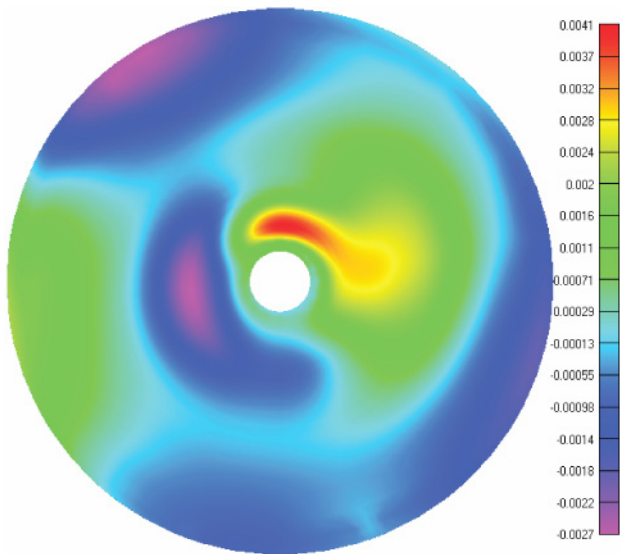


Figure 11. Typical reflector surface normal deformation from finite element analysis, corresponding to the temperatures in Figure 10. Deformation is relative to best-fit rigid body motion. Units are inches.

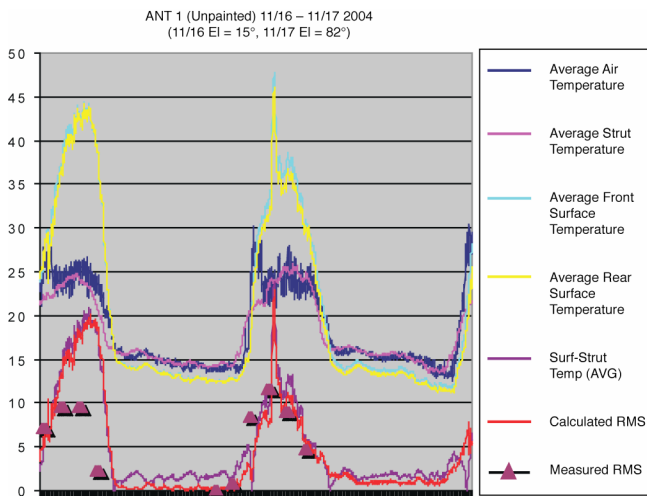


Figure 12. Antenna #1 (Unpainted) Temperatures and Distortions

front surface and struts was considerably smaller than the unpainted configuration. Again, the distortion tracked this difference for both the calculated and measured rms. The rms of the painted dish is less than one half of the unpainted dish.

A second 6-meter antenna, Antenna #2, was painted and installed on the JPL Mesa antenna range nearby Antenna #1 (see Figure 14). The same types of measurements were taken with the antenna pointed in elevation at 15 degrees, 45 degrees and 82 degrees on each of three days. The data are plotted in Figures 15 to 17. Observe that the performance is very nearly the same as painted Antenna #1. For all cases measured for both the painted Antenna #1 and

the rms due to thermal effects is less than the required 5 mils.

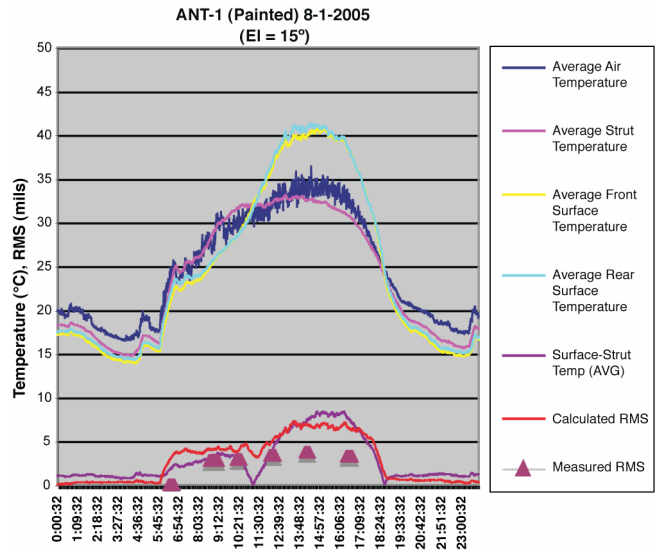


Figure 13. Antenna #1 (Painted) Temperatures and Distortions



Figure 14. Antenna #1 and Antenna #2 on the Mesa Antenna Range

7. PROPOSED 12-METER HYDROFORMED REFLECTOR FOR US SKA

The square kilometer array (SKA) is an international project that will be the next big step in radio astronomy. As the name indicates the radio telescope will have a staggering total aperture area of about 1 square kilometer. The US proposal makes use of an array of around 5000 symmetric parabolic reflectors with 16 m diameter, consisting of a 12-meter diameter hydroformed shell and a 2-meter mesh extension. A sketch of the proposed symmetric reflector is

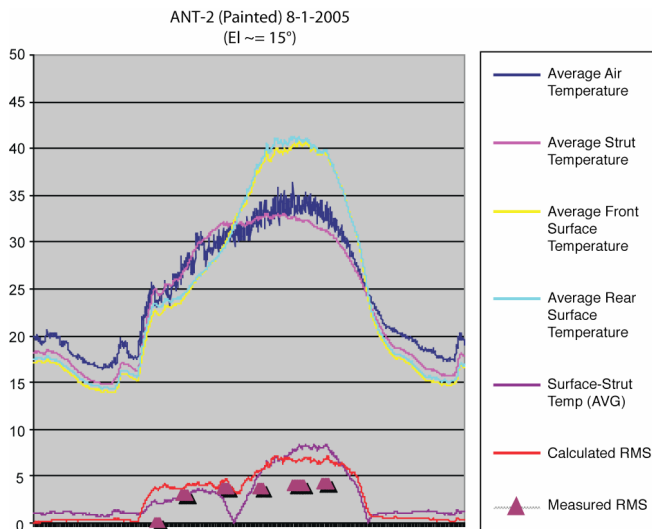


Figure 15 Antenna#2 (Painted) Temperatures and Distortions at 15 degrees Elevation Angle

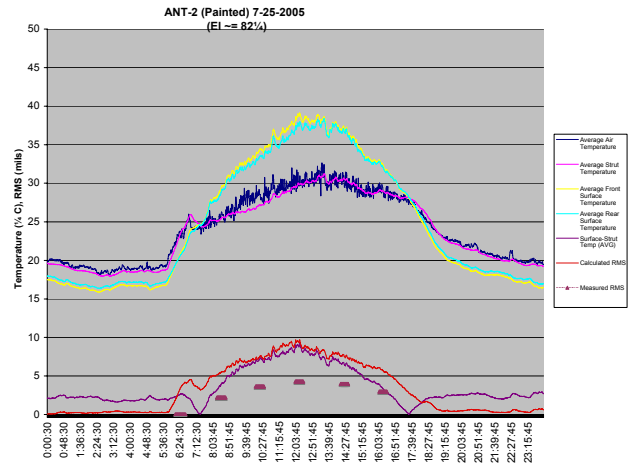


Figure 17. Antenna#2 (Painted) Temperatures and Distortions at 82 degrees Elevation Angle

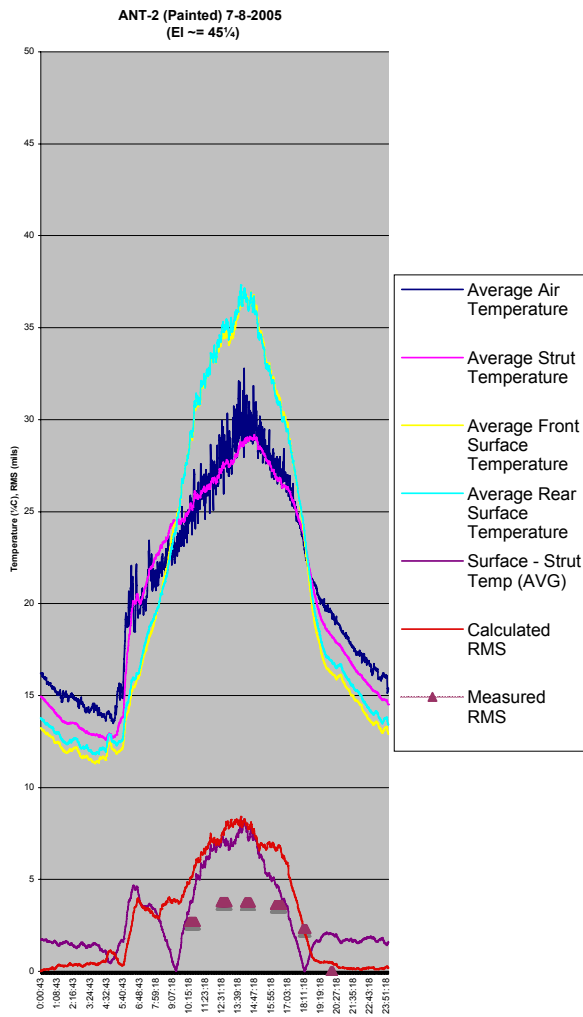


Figure 16. Antenna#2 (Painted) Temperatures and Distortions at 45 degrees Elevation Angle

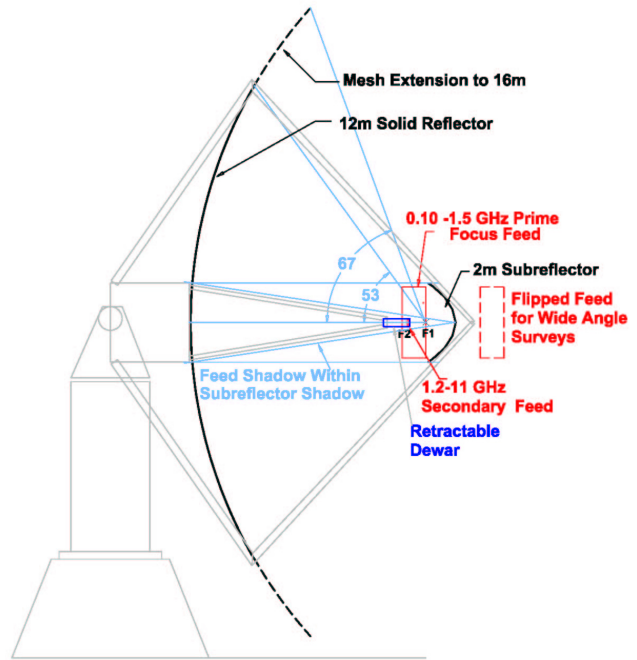


Figure 18. US SKA 12m/16m Antenna Concept

shown in Figure 18. One of the advantages with the US proposal is that it makes use of reflector antennas that represent a well-known technology, which has been used in radio astronomy during several decades. The system is very wide band; the goal is to cover 100 MHz to 25 GHz. It will use a 2-meter Gregorian subreflector and have a feed mounted on the back of the subreflector that can be used for wide angle surveys or flipped in front for use as a prime focus feed. At the secondary focus are feeds that will operate up to 25 GHz. One concern for the high frequency operation is the thermal distortion performance.

The proposed design is scaled up from 6-meter concepts. However there are difficulties that arise from only scaling the design concept upward. These difficulties and a first

solution are enumerated as follows. Spar lengths become structurally unmanageable from the perspective of length over radius of gyration, the measure of column stability (Euler).

The JPL 6-meter antennas had the rim supporting spars terminated in two work points behind the reflector, which straddled the mount. These points were so far behind the reflector such that opposite pairs of spars generally made a right angle between each other at these rear work points. The 12-meter reflector could not be shipped down highways in most parts of the world as the 6-meter could. The proposed design as shown in Figure 19 can alleviate all of the above problems. Spars are replaced by radial truss structures emanating from a center hub with manageable span lengths. These radial trusses are integrated into the shell in the sense that the truss members closest to the reflector shell are formed and stabilized partly by that shell. The reflector is split for shipping at least along a plane thru the RF axis and the center plane transverse to the elevation axis. With this split and the radial truss depth set as it is, one half of a 12-meter reflector can go down the highway thru underpasses with a permit in many parts of the world.



Figure 19. Mechanical Configuration of US SKA Antenna

8. THERMAL DESIGN

Deflections due to thermal gradients were calculated. Several challenges arise when producing this analysis; 1) Assessment of realistic convective heat loss to the air in real wind spectra, 2) acquiring solar heating weighted reflectance and IR re radiation emissivity, 3) grooming of

the model to apply meaningful heat transfer parameters representing all significant elements of convection and radiation, 4) assessment of the solar heating incidence on a statistical basis at all the geographic locations as yet unpicked and surveyed and 5) Resolving the sun's heating to the myriad surfaces of the model. A steady state analysis was utilized to assess the temperature distribution in the reflector.

Convective heat transfer coefficients were first conservatively taken from textbooks listing formulation for dead calm air. Resulting temperature distributions contained differentials between the hottest and coolest parts of the model were much higher than observed over many days in the temperature survey by Lamb and Woody described in Reference [4].

The convective heat transfer coefficients were then adjusted upward to the point where the resultant peak temperature difference was reduced to the least prevalent difference observed by Lamb and Woody, 9 deg. C, if the reflectance of their white paint was as good as high reflectance Triangle paint.

Figure 20 shows the complexity of the meshed shell model. Care was required to place the numerous "split lines" which divide the surfaces in such a way that the automatically generated mesh nodes at joined edges behave in a connected way during the analysis. This happens when nodes are co-located; particularly at edges where three shells come together edgewise. The solar heating was assessed facet by facet. Worst-case assumptions for clear desert air incidence are discounted for latitude and the cosine assuming the dish is face on to the sun.

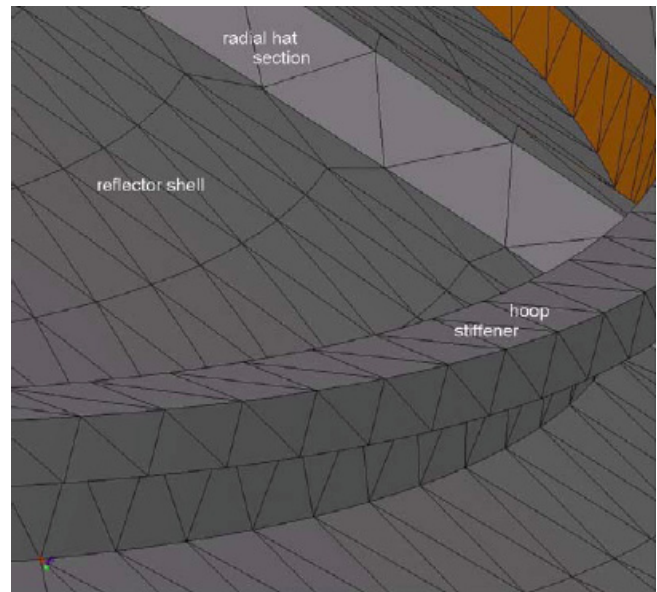


Figure 20. Mesh Node Connectivity at Three Way Edge Intersections

Face on sun represents one of the extreme thermal cases. It was calculated to be representative of thermal distortion. Other cases where sun incidence is off the RF axis are very much more complex to apply to the model and will be examined in the future.

9. THERMAL RESULTS

A calculation of representative surface finishes versus rms surface error is shown in Table 2. Only the inorganic high reflectance coating produces an acceptable rms error for operation at 25 GHz.

Figure 21 shows a representative temperature distribution for the inorganic high reflectance coating (IHRC). The highest temperature is 6.87 deg F (3.8 deg C) above ambient.

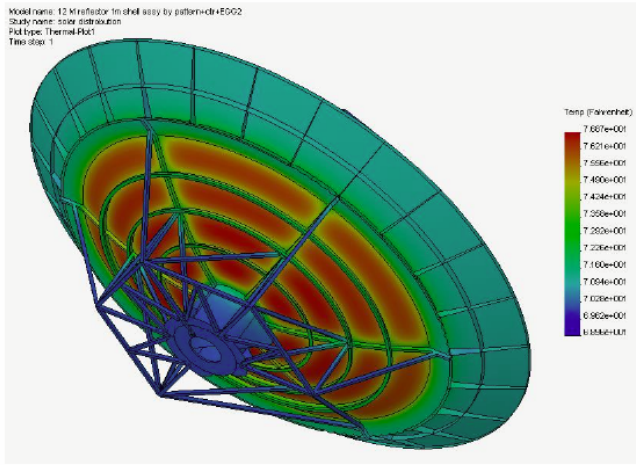


Figure 21. Calculated Temperature Distribution, IHRC

Figure 22 shows the temperature distribution near a radial hat section. Here we see that there is a smooth transition from the back structure cooling to the high temperature at the middle of the reflector shell between the supports.

Figure 23 shows the residual error in the reflector surface after best fitting for IHRC. It is clear from this plot that the most significant errors accrue due to the gradient shown in Fig. 21. Ongoing design efforts will be directed at reducing these local phenomena.

It is clear, as with the 6-meter antenna, that temperature difference governs surface accuracy as shown in Fig. 24.

Since thermal distortion is proving to be the most challenging issue for the US SKA reflector, several combinations of solar heating weighted reflectance and re radiation IR emissivity were analyzed and shown in Fig. 25 to understand the overall impact of these parameters. Some

data points represent attainable combinations; others are included to complete the two emittance curves.

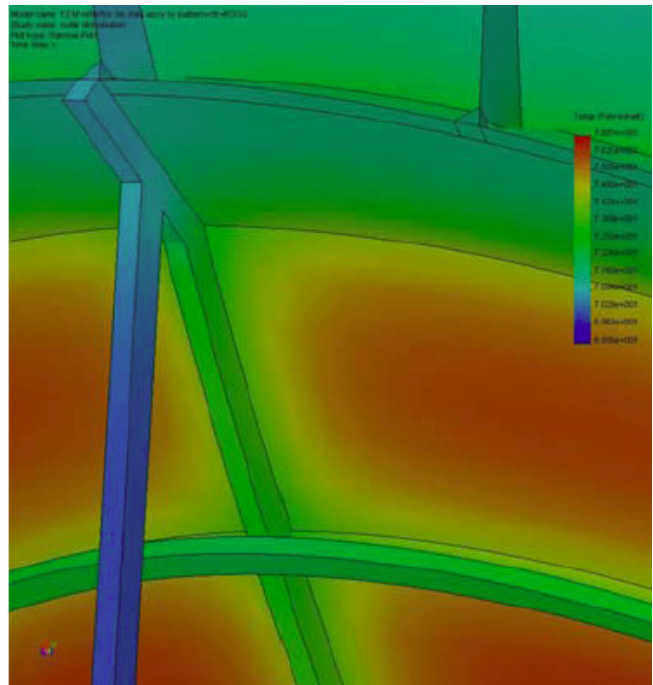


Figure 22. Temperature Gradients Near Back Structure Detail

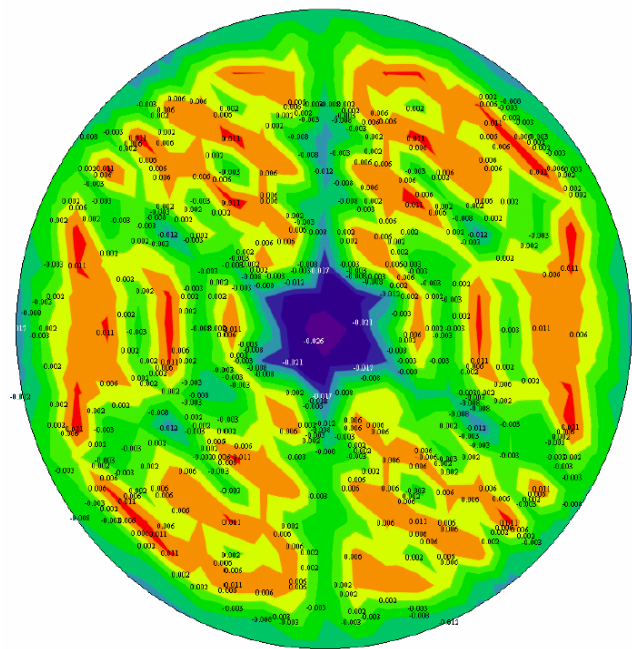


Figure 23. Best-Fit Errors for the IHRC Coated Reflector

Table 2 Surface Finish versus rms Surface Error

Surface Finish vs RMS Surface Error	Solar Heating Reflectance	Re-radiation IR Emittance	Thermal surface error in. RMS	Max Temperature Differential, deg. F
Unfinished aluminum-aged	71.3%	0.05	0.104	101.6
Insil-tec white paint	77.8%	0.9	0.03699	33
Triangle high reflectance white paint	85.0%	0.91	0.0218	16.56
Inorganic high reflectance coating IHRC	95.0%	0.4	0.00782	6.87

Temperature difference governs surface accuracy

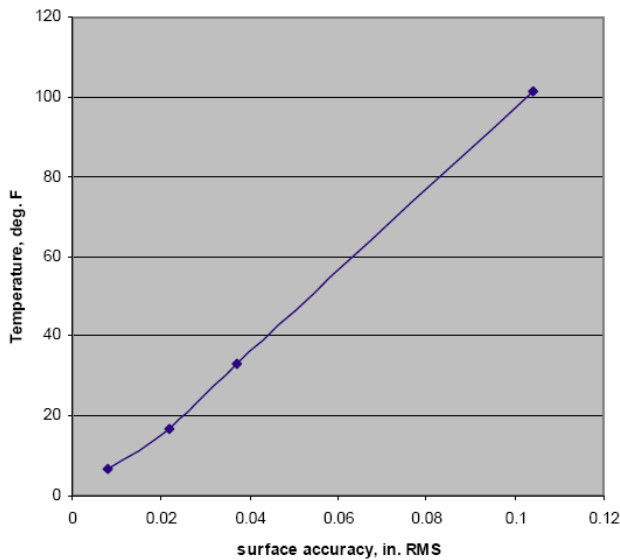


Figure 24. Surface Error vs. Temperature Differential, deg. F

10. CONCLUSIONS

A low cost 6-meter antenna made with a hydroformed shell for a main reflector was demonstrated to be very stiff (excellent performance versus elevation angle) and thermally very stable when painted with triangle no. 6 diffusive white paint. A design was proposed to extend the shell diameter to 12-meters and a backup structure and surface finish that would meet the required SKA specifications was shown.

ACKNOWLEDGMENT

The research was carried out at the Jet Propulsion Laboratory, California Institute of Technology, under a contract with the National Aeronautics and Space Administration.

REFERENCES

- [1] M. S. Gatti, "The Deep Space Network Large Array," *The Interplanetary Network Progress Report*, vol. 42-157, Jet Propulsion Laboratory, Pasadena, California, pp. 1-9, May 15, 2004.
[http://ipnpr/progress report/42-157/157O.pdf](http://ipnpr/progress%20report/42-157/157O.pdf)
- [2] Square Kilometer Array, the international Radio Telescope for the 21st century,
<http://www.skatelescope.org/>
- [3] W. A. Imbriale, S. Weinreb, A. Fera, C. Porter, D. Hoppe, and M. Britcliffe, "The 6-Meter Breadboard Antenna for the Deep Space Network Large Array," *The Interplanetary Network Progress Report*, vol. 42-157, Jet Propulsion Laboratory, Pasadena, California, pp. 1-12, May 15, 2004.
[http://ipnpr/progress report/42-157/157M.pdf](http://ipnpr/progress%20report/42-157/157M.pdf)
- [4] J. W. Lamb and D. P. Woody, "Thermal Behavior of the Leighton 10-m Antenna Backing Structure," NRAO/ALMA web site MMA memo 234 found at
http://www.ovro.caltech.edu/~lamb/ALMA/Antenna_memos.htm

**Thermal Surface Accuracy, Natural Convection "3 sigma calm"
USSKA Strawman 12-16 meter antenna**

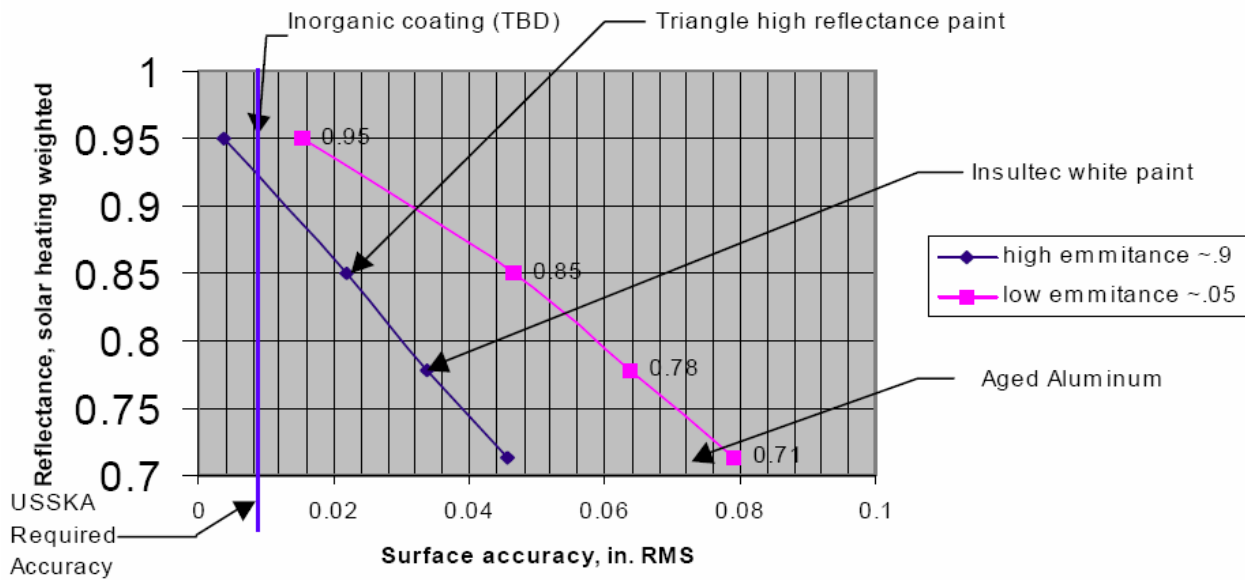


Figure 25 Surface Error vs. Solar Heating Reflectance and IR Emittance

BIOGRAPHY

William A. Imbriale is a senior research scientist in the Communications Ground System Section at the Jet Propulsion Laboratory (JPL) in Pasadena, California. Since starting at JPL in 1980, he has led many advanced technology developments for large ground-station antennas, lightweight spacecraft antennas, and millimeter-wave spacecraft instruments. He has recently returned from a 6 month sabbatical at CSIRO in Australia where he worked with the Australian Telescope National Facility. He is currently working on the Deep Space Network Large Array, a concept to significantly increase the capability of the Deep Space Network (DSN) by arraying a large number of inexpensive small antennas. Earlier positions at JPL have included being the Assistant Manager for Microwaves in the Ground Antennas and Facilities Engineering Section and the Manager of the Radio Frequency and Microwave Subsystem Section.

Prior to joining JPL in 1980, Dr. Imbriale was employed at the TRW Defense and Space Systems Group where he was the Subproject Manager for the Antennas of the TDRSS program.

Dr. Imbriale is a Fellow of the IEEE and has an extensive list of publications.



Eric Gama is a member of the engineering staff in the Communications Ground System Section at the Jet Propulsion Laboratory (JPL) in Pasadena California. A graduate of the California State University Los Angeles School of Engineering and Technology, he has a Bachelor of Science degree in Mechanical Engineering.

Starting in 1998 at JPL as an academic part time (APT) employee, he has worked on the research and development of gossamer structures as a way of reducing launch payload and volume, for use on space deployable, reflect-array antennas. Since beginning his full-time status at JPL, he has been part of the Antenna Mechanical and Structural Engineering Group responsible for the mechanical design and maintenance of the large aperture antennas of NASA's Deep Space Network (DSN).



Dr. Smith is a Senior Scientist at Alliance Spacesystems, Inc. His primary expertise is in structural dynamics analysis and testing for space structures. He previously worked at the Jet Propulsion Laboratory,



where he was responsible for launch loads analysis for the Cassini mission to Saturn, and entry/descent/landing analysis for the Mars Pathfinder mission.

Mr. Schultz levers nearly 40 years of experience designing and developing new economical antenna structures and axis drive mechanisms using a realistic and proven understanding of engineering mechanics, dynamic analysis and FEA, concept through sell off.

